Neutron Star Astrophysics at the Crossroads: Magnetars and the Multimessenger Revolution
Proceedings IAU Symposium No. 363, 2023
E. Troja & M. G. Baring, eds.
doi:10.1017/S1743921322000473

Novel Clues to the Physics of Magnetars as Probed with Detailed Pulse-Timing Studies

Kazuo Makishima

[1]Kavli IPMU, University of Tokyo, 5-1-5 Kashiwa-no-ha, Kashiwa, Chiba, Japan, 277-8583
email: maxima@phys.s.u-tokyo.ac.jp

[2]Dept. of Physics, University of Tokyo, 7-3-1 Hong, Bunkyo-ku, Tokyo, Japan, 113-0033

Abstract. Broadband X-ray data of five magnetars show that their hard X-ray pulses suffer periodic phase modulations, at a period $\sim 10^4$ times their pulse period. The phenomenon is interpreted as a result of free precession of neutron stars that are prolately deformed to an asphericity of $\sim 10^{-4}$, by the magnetic stress of toroidal fields reaching $\sim 10^{16}$ G. The behavior is absent in their soft X-ray pulses, probably due to a higher emission symmetry. The ultra-high toroidal fields, considered common to magnetars, may persist longer than their dipole fields.

Keywords. Magnetars; Astrophysical magnetism; Neutron stars; Pulsars; X-ray sources

1. Introduction

X-ray spectra of magnetars generally consist of the soft X-ray component (SXC) and the hard X-ray component (HXC), which dominate typically in < 10 keV and > 10 keV, respectively. As in Fig. 1, the SXC pulses of magnetars, reflecting the spin of the neutron stars (NSs), are easily detectable, but those in the HXC often remain insignificant when we rely on the conventional epoch-folding plus Z^2 statistics searches. As we have revealed so far, this is because the HXC pulses of magnetars are very often subject to slow phase modulations, at a period $T \sim 10^4 P$ (Makishima *et al.* 2014, 2016, 2014, 2021a, 2021b), where P denotes the pulse period. Since this effect is presumably caused by the magnetic deformation of NSs, its study will provide valuable clues to the magnetars' ultra-strong toroidal magnetic field $B_{\rm t}$, which cannot be easily studied with other means.

2. Data Analysis and Results

The phenomenon of pulse-phase modulation (PPM) can be studied by "demodulation" analysis, assuming that the arrival time t of each photon is periodically modulated as

$$\delta t = A \sin(2\pi t/T - \psi_0). \qquad (2.1)$$

Here, T, A, and ψ_0 are the period, amplitude, and initial phase of the assumed PPM, respectively. By optimizing the triplet (T, A, ψ_0), we examine whether the pulse significance improves at a period that is consistent with the SXC period.

Figure 2 shows a basic tool, called a demodulation diagram (DeMD), which quantifies the pulse significance (in Z_4^2, after optimizing P, A, and ψ_0) as a function of T. We used archival data from *Suzaku*, *NuSTAR*, and *ASCA*. In the HXC signals of all five objects, we have thus detected a clear DeMD peak, which implies a significant PPM.

We summarize the results of data analyses in Table 1. The five objects consistently show the following PPM properties, suggesting a common physics working in them.

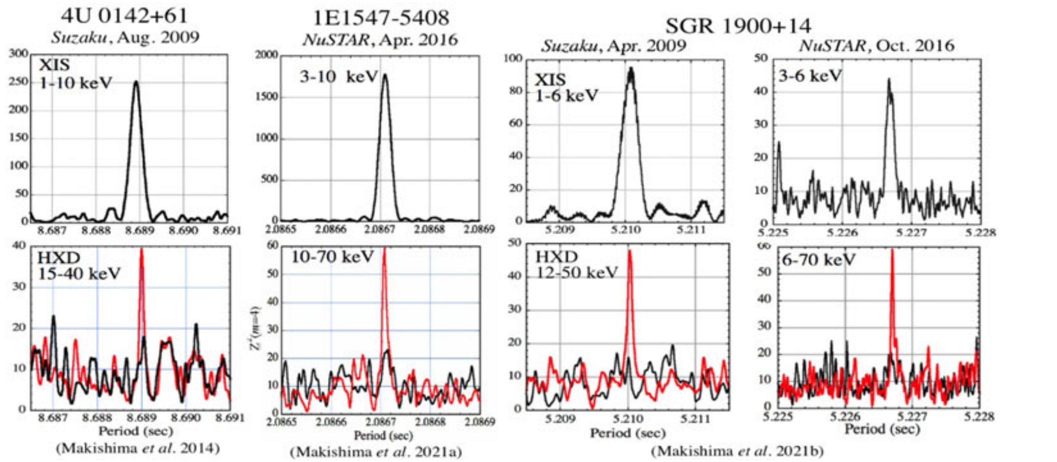

Figure 1. Pulse periodograms of three magnetars, derived with the epoch-folding and Z_4^2-evaluation method. The top row is for the SXC, and the bottom row is for the HXC where black and red traces indicate before and after the demodulation via eq.(2.1), respectively.

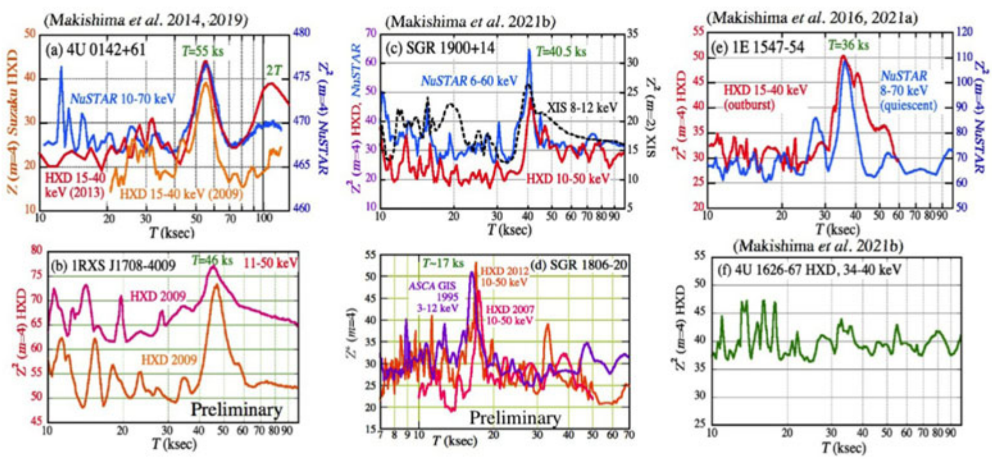

Figure 2. DeMDs of five magnetars. The abscissa is the assumed modulation period T, and the ordinate the maximum pulse significance in Z_4^2 when A, ψ_0, and P are optimized.

Table 1. Summary of the detected HXC PPMs.

Object	Type	Observation	P (sec)	T (ksec)	P/T (10^{-4})	B_d $(10^{12}$ G)	References
4U 0142+63	AXP	*Suzaku* 2009	8.68899	55 ± 2	1.6	1.3	Makishima+14
		Suzaku 2013	8.68914				Makishima+14
		NuSTAR 2014	8.68917				Makishima+19
1E 1547−54	Tran.	*Suzaku* 2009	2.072135	36 ± 3	0.6	3.2	Makishima+16
		NuSTAR 2016	2.086712				Makishima+21a
SGR 1900+14	SGR	*Suzaku* 2009	5.21003	40.5 ± 0.5	1.3	7.0	Makishima+21b
		NuSTAR 2016	5.22670				Makishima+21b
1RXS J1708−4009	AXP	*Suzaku* 2009	11.00623	46 ± 2	2.4	4.7	in prep.
		Suzaku 2010	11.00701				
SGR 1806−20	SGR	*ASCA* 1995	7.4738	17 ± 1	4.5	20	in peer.
		Suzaku 2007	7.6026				
		Suzaku 2015	7.7497				

https://doi.org/10.1017/S1743921322000473 Published online by Cambridge University Press

1. The PPM is generally significant in each data set, even considering various timing noise and intensity variations therein (Makishima *et al.* 2014, 2016).
2. The PPM effect is seen in the HXC, but absent in the SXC. Therefore, it cannot originate from orbital Doppler effects.
3. The value of T is specific to each object with a good reproducibility. However, the insufficient accuracies in the individual T determinations (Table 1) hamper us to coherently phase connect the PPMs across different data sets of each object.
4. In each object, A varies from time to time over a range of $(0.02-0.25)P$.
5. We find $P/T \sim 10^{-4}$ in all cases, and obtain $B_{\rm t} \sim 10^{16}$G if eq.(3.3) in § 3.2 is used.
6. As shown by Makishima *et al.* (2021a) and (2021b), often ψ_0 and A are energy dependent, possibly due to some strong-field physics.
7. Via demodulation, the pulse profiles in different energy ranges come into a better alignment, and often exhibit 3 to 4 peaks per cycle.

In addition, a further study of SGR 1806−20, with its rapid spin down and the short T, may allow us to observationally verify the expectted $T \propto P$ relation.

3. Discussion

3.1. *Interpretation of the PPM*

As we developed in our series of publications from Makishima *et al.* (2014) to Makishima *et al.* (2021b), the results described above are interpreted in the following way. According to Ioka & Sasaki (2004), strong $B_{\rm t}$ will axially elongate the NS to an asphericity of

$$\epsilon \equiv \delta I/I \sim 10^{-4}\left(B_{\rm t}/10^{16}{\rm G}\right)^2 . \tag{3.1}$$

Such a NS performs free precession, in which the symmetry axis $\hat{x}_3$ rotates around the angular momentum vector, with a period $P_{\rm fp}$ and a wobbling angle α. The star also rotates around $\hat{x}_3$, with a period $P_{\rm rot} = P_{\rm rot}/(1+\epsilon)$. When the NS emission is symmetric around $\hat{x}_3$, we can detect $P_{\rm fp}$ as the pulsation, but cannot observe $P_{\rm rot}$. If, in contrast, the emission breaks the symmetry around $\hat{x}_3$ either positionally or directionally, the pulse phase becomes modulated at the beat period (called slip period) between $P_{\rm fp}$ and $P_{\rm rot}$, to be identified with the modulation period and is given as

$$T = P_{\rm fp}/\epsilon\cos\alpha. \tag{3.2}$$

The difference between the SXC and HXC may be explained if the SXC is emitted with a better axial symmetry around $\hat{x}_3$ than the HXC which is presumably beamed strongly. Because neither T nor α would change on short time scales, the observed changes in A may result from variations in the HXC anisotropy (Makishima *et al.* 2021a).

Makishima *et al.* (2021b) examined some alternative interpretations of the PPM, assuming that magnetars are isolated NSs accreting from fossil disks. However, such scenarios were found difficult to explain the overall results described here.

3.2. *Estimation of* $B_{\rm t}$

From eq.(3.1) and eq.(3.2), and assuming $\cos\alpha \sim 1$, we can estimate $B_{\rm t}$ as

$$B_{\rm t}/10^{16}{\rm G} \sim \sqrt{10^4\epsilon} = \sqrt{10^4 P_{\rm fp}/T\cos\alpha} \sim \sqrt{10^4 P_{\rm fp}/T}. \tag{3.3}$$

The values of $B_{\rm t}$ thus estimated for the 5 magnetars, normalized to their dipole magnetic filed $B_{\rm d}$ (derived in the usual way and given in Table 1), are shown in Fig. 3 against their characteristic age $\tau_{\rm c}$. It suggests a scaling as $B_{\rm t}/B_{\rm d} \propto \tau_{\rm c}^{0.36}$. Magnetars are hence suggested to keep their toroidal (internal) field longer than the dipole field. We then expect a large population of old magnetars, of which $B_{\rm d}$ has already decayed but $B_{\rm f}$

https://doi.org/10.1017/S1743921322000473 Published online by Cambridge University Press

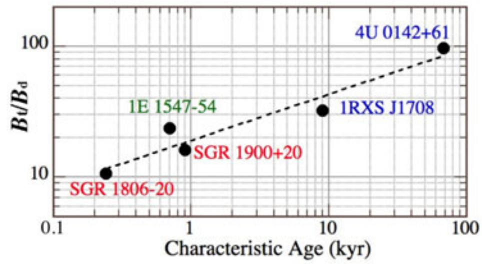

Figure 3. The toroidal magnetic fields B_t of the five magnetars, estimated with eq.(3.3) and normalized to their dipole field B_d. The abscissa shows the characteristic age, and the dashed line represents a logarithmic slope of 0.36.

remains still high. These may explain such NSs subclasses as Central Compact Objects and X-ray Dim Isolated NSs, and support the view by Nakano *et al.* (2015) that a considerable fraction of NSs are born as magnetars, which then become quickly invisible.

3.3. *A counter example*

To remove a concern that the PPM might appear in any NS, we also analyzed the *Suzaku* HXD data of the binary pulsar 4U 1626−67; its pulse period (7.7 s) is similar to those of magnetars, and its orbital Doppler effect is negligibly small (<13 lt-msec). As described in Makishima *et al.* (2021b) and given in Fig. 2 (f), no evidence of PPM was detected. Thus, the phenomenon studied here is considered specific to the HXC of magnetars, and is expected to provide important knowledge on the physics of strong ($\gg 10^{12}$ G) magnetic fields. We do not, however, mean that magnetars are absent in binaries. As revealed by Yatabe *et al.* (2016) and Yoneda *et al.* (2000), the long-period binary pulsar X-Persei and the MeV-brightest gamma-ray binary LS 5039 are likely to host magnetars.

4. Conclusion

1. Magnetars are thought to ubiquitously harbor $B_t \sim 10^{16}$ G, and prolately deformed to $\epsilon \sim 10^{-4}$. As a result, they perform free precession.
2. The HXC emission is thought to break the axial symmetry. Coupled with the free precession, this causes the HXC pulses to be phase-modulated at the slip period.
3. The axial asymmetry of the HXC emission changes with time, and the degree of its asymmetry may be considerably energy dependent.
4. The absence of soft X-ray PPM suggests that the SXC emission is more symmetric around $\hat{x}_3$ than the HXC. Thus, the two components have distinct origins.
5. The toroidal fields of magnetars may persist longer than their dipole fields.

References

Ioka, K., & Sasaki, M. 2004, *ApJ*, 600, 296

Makishima, K. 2016, *Proc. Japan Academy, Ser. B*, 92, 135

Makishima, K., Enoto, T., Hiraga, J. S., Nakano, T., *et al.* 2014, *Phys. Rev. Lett.*, 112, id.171102

Makishima, K., Enoto, T., Murakami, H., Furuta, Y., Nakano, T., *et al.* 2016, *PASJ*, 68S, id.12

Makishima, K., Murakami, H., Enoto, T., & Nakazawa, K. 2019, *PASJ*, 71, id.15

Makishima, K., Enoto, T., Yoneda, H., & Odaka, H. 2021a, *MNRAS*, 502, 2266

Makishima, K., Tamba, T., Aizawa, Y., Odaka, H., Yoneda, H., *et al.* 2021b, *ApJ*, 923, id.63

Nakano, T., Murakami, H., Makishima, K., Hiraga, J. S., *et al.* 2015, *PASJ* 67, id.9

Yatabe, F., Makishima, K., Mihara, T., Nakajima, M., *et al.* 2016, *PASJ*, 70, id.89

Yoneda, H., Makishima, K., Enoto, T., *et al.* 2020, *Phys. Rev. Lett.*, 125, id.111103

https://doi.org/10.1017/S1743921322000473 Published online by Cambridge University Press